WRINKLE RIDGES AND ANCIENT RIFTS BORDERING PROCELLARUM AND FRIGORIS IDENTIFIED IN GRAIL GRAVITY DATA. T. R. Watters[1], D.R. DeFelice[1, 2], [1]Center for Earth and Planetary Studies, National Air and Space Museum, Smithsonian Institution, Washington, DC 20560, USA (watterst@si.edu); [2]Department of Geology and Astronomy, West Chester University, West Chester, PA 19383, USA.

Introduction: The recent and current stress state of the Moon is dominantly contractional. This is evident from a vast population of globally distributed lobate thrust fault scarps revealed in images returned from the Lunar Reconnaissance Orbiter Camera (LROC) [1-3]. The period of dominant global contraction appears to date back as far as ~3.6 Gyr when large-scale mare basin-related extension appears to have ceased [4-7], marking a stage in the Moon's thermal history at which interior cooling resulted in a shift from net expansion to net contraction [8, 9]. During the last stages of this period of net expansion, starting at ~3.9–4.0 b.y., the mare basalts were emplaced [10]. Coincident with and following their emplacement, mare basalts were deformed by contractional tectonics in the form of wrinkle ridges [11]. Wrinkle ridges occur in the interiors and near the basin-margins and are often accompanied by graben at the margins or exterior to the mare basins. The spatial distribution of wrinkle ridges and graben and their association with positive free-air gravity anomalies is the basis for the mascon tectonic model [12, 13]. The accumulation of mare basalts on an impact-thinned and weakened lithosphere results in load induced flexure and subsidence, causing contraction in the interior of the basin and extension near the margins [12, 13]. Complex patterns of wrinkle ridges have been revealed in recent global surveys using LROC WAC and NAC images and mosaics and WAC stereo derived topography [e.g., 14, 15] (Fig. 1). Perhaps most intriguing are the complex patterns that have emerged in the non-mascon mare such as Mare Frigoris and Procellarum.

Ancient Rifts: Unprecedented resolution global gravity field maps of the Moon have been provided by the Gravity Recovery and Interior Laboratory (GRAIL) mission [16-18]. Numerous previously unresolved features in the lunar crust have been revealed including tectonic structures and volcanic landforms [16]. Prominent narrow linear anomalies that border Procellarum and Mare Frigoris apparent in GRAIL Bouguer gravity gradient maps [19] are interpreted to be a pattern of rift valleys formed when the Procellarum KREEP Terrane (PKT) cooled and contracted, resulting in extension at its margins [20]. It it suggested that this ancient rift system was flooded by mare basalt. Accompanying dyke intrusion may have supplied magma that filled the nearside mare basins and lowlands. Andrews-Hanna et al. [20] speculate that filling of the rifts resulted in load-induced flexure and contraction that inhibited further magma ascent and localized wrinkle ridges with orientations that parallel the buried rifts [20]. They also suggest that wrinkle ridges over and parallel- ing the bordering rifts may express structural control by these buried features.

Wrinkle Ridges of Procellarum and Frigoris: The distribution of wrinkle ridges mapped using LROC mosaics and stereo derived topography indicates a direct spatial correlation with segments of the narrow linear Bouguer and gradient anomalies (Fig. 1). A large number of the wrinkle ridges that occur outside the mascon basins are spatially associated with the anomalies. The hypothesis that co-located wrinkle ridges have been controlled by subsurface structures related to buried border rifts can be tested by examing the displacement-length (*D/L*) of wrinkle ridges within and outside areas delineated by the GRAIL Bouguer gradient anomalies. Fault displacement scales with length as a linear function such that $D = \gamma L$, where γ is a constant governed by mechanical properties and tectonic setting [e.g., 21, 22]. Analysis of the D_{max} and L for 26 co-located ridges and 34 ridges outside zones defined by the gradient maps in Procellarium and Frigoris using LROC image mosaics and stereo-derived DTMs have been made. The values of γ for both populations of wrinkle ridges are nearly identical at $\cong 6.1\times10^{-3}$ for $\theta = 30°$ (Fig. 2). Thus, no significant difference in the distribution of maximum displacement or lengths of the measured ridges within and outside of the anomalies is evident. The linear scaling relationship (Fig. 2) indicates that the growth of the analyzed thrust faults was not restricted by other influences [23], like subsurface structures. Restricted fault growth can be expressed by nonlinear paths that deviate significantly from unrestricted growth trends. Thus, there is no evidence the co-located ridges were influenced by buried structures related to ancient rifts.

Elevation Offset Ridges: Evidence of restricted growth is found in the *D/L* relationship of the mare ridges with large elevation offsets (EO). This class of wrinkle ridge occurs in mascon basins, exclusively near the basin margins, and with the offset on the interior-side of the ridge. Large elevation offsets have been cited as evidence of deeply rooted thrust faults [24, 25]. The *D-L* values of these wrinkle ridges do not fall along the trend defined by the population of mare ridges in Procellarum and Frigoris (Fig. 2). The observed deviation may reflect restricted growth of the EO ridge thrust faults due to the influence of subsurface basin structure. Large impact basins are characterized by peak-rings and down-dropped blocks forming terraced zones [see 26]. The sensitivity of wrinkle ridges to shallow mechanical discontinuities such as buried impact craters (i.e., ghost craters) suggests that the EO ridges were controlled by shallow thrust

faults localized by buried peak rings or reactivated normal faults formed during transient crater collapse. Thus, EO ridges may not be the result of deeply rooted, unrestricted thrust faults.

References: [1] Robinson, M.S. et al. (2010) *Space Science Reviews, 150*, 81–124, doi:10.1007/s11214-010-9634-2. [2] Watters T.R. et al. (2010) *Science*, *329*, 936-940. [3] Watters T.R. et al. (2015) *Geology*, *43*, 851–854. [4] Lucchitta, B.K. and Watkins, J.A. (1978) *Proc. Lunar Planet. Sci. Conf. 9*, 3459-3472. [5] Boyce, J. M. (1976) *Proc. Lunar Planet. Sci. Conf. 7*, 2717-2728. [6] Hiesinger, H. et al. (2000) *J. Geophys. Res.*, *105*, 29239-29276. [7] Hiesinger H. et al. (2003) *J. Geophys. Res.*, *108*, 5065. [8] Solomon, S.C. and Head, J.W. (1979) *J. Geophys. Res.*, *84*, 1667-1682. [9] Solomon, S.C. and Head, J.W. (1980) *Rev. Geophys. Space Phys., 18*, 107-141. [10] Hiesinger H. et al. (2012) *Geol. Soc. Am. Special Paper 477*, 1-51, doi: 10.1130/2011.2477(01). [11] Watters T.R. and Johnson C.L. (2010) in *Planetary Tectonics*, Cambridge Univ. Press, pp. 121-182. [12] Melosh, H. J. (1978) *Proc. Lunar Planet. Sci. Conf. 9*, 3513-3525. [13] Freed, A. M. et al. (2001) *J. Geophys. Res.*, *106*, 20603-20620. [14] Yue Z. et al. (2015) *J. Geophys. Res.*, *120,* 978-994. [15] Thompson, T.J. et al. (2017) *LPSC 48*, 2665. [16] Zuber, M. T., et al. (2013) *Science*, *339*, 668-671. [17] Konopliv, A. S., et al. (2013) *J. Geophys. Res., 118*, 1415-1434. [18] Lemoine, F. G., et al. (2013) *J. Geophys. Res., 118*, 1676-1698. [19] Lemoine, F. G., et al. (2014) *Geophys. Res. Letts., 41*, 3382-3389. [20] Andrews-Hanna J.C. et al., (2014) *Nature*, *514*, doi:10.1038/nature13697. [21] Cowie, P. A. and Scholz, C. H. (1992a) *J. Struct. Geol., 14*, 1133-1148. [22] Cowie, P. A. and Scholz, C. H. (1992b) *J. Struct. Geol., 14*, 1149-1156. [23] Schultz, R. A. et al. (2010), *in Planetary Tectonics*, Cambridge Univ. Press, pp. 457–510. [24] Golombek, M. P. et al. (1991) *Proc. Lunar Planet Sci. Conf. 21*, 679-693. [25] Byrne, P.K. et al. (2015) *EPSL, 427*, 183-190. [26] Baker, D.M.H. et al. (2013) *Icarus*, *273*, 146-163.

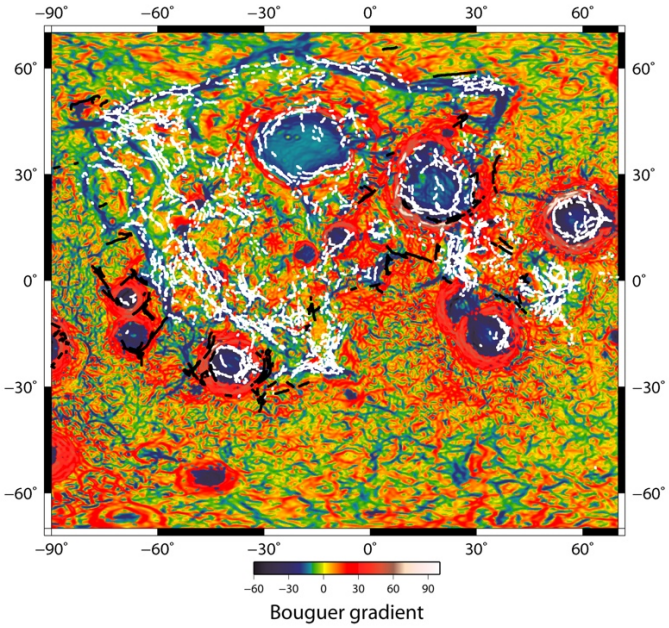

Figure 1. GRAIL Bouguer gravity gradient map with tectonic landforms. The gradient map was derived from the GRGM900C field model (units are Eötvös) [19]. Wrinkle ridges (white lines) are collocated with roughly linear border gradient anomalies. The mascon mare appear as dark blue circular features. Wrinkle ridges plotted are those with digitized segment lengths >10 km along with basin related extensional graben (black lines). The GRAIL Bouguer gravity gradient map was provided by Sander Goossens and Erwan Mazarico.

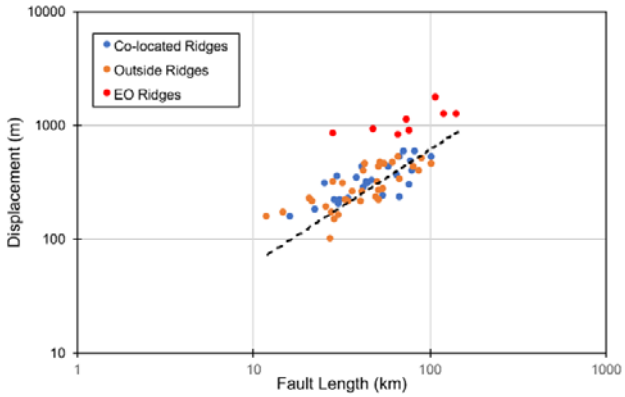

Figure 2. Log-log plot of maximum displacement as a function of fault length for wrinkle ridges in Mare Procellarium and Mare Frigoris and elevation offset ridges. Co-located ridges are spatially associated with GRAIL Bouguer gravity gradient anomalies bordering Procellarium and Frigoris (see Fig. 1). Outside ridges are not spatially co-located with the gradient anomalies. Elevation offset (EO) ridges are located in mascon mare basins and are not found in Procellarium and Frigoris.